Structure-Property Correlations in ZnO Tetrapods and Spheres prepared by Chemical Vapour Synthesis

Revathi Bacsa[*], Yolande Kihn[**], Marc Verelst[**], Jeannette Dexpert[**], Wolfgang Bacsa[**] Philippe Serp[*]

[*] Laboratoire de Chimie de Coordination, Composante ENSIACET, 118 Route de Narbonne Toulouse 31077, France, Revathi.Bacsa@ensiacet.fr

[**]CEMES CNRS UPR, 29 rue Jeanne Marvig, Univ. Toulouse, 31055 Toulouse France

ABSTRACT

We present experimental results on the synthesis and characterization of ZnO nanorods, tetrapods and nanospheres prepared by the gas phase oxidation of zinc vapor followed by the collection of the oxide particles in an aerosol. Spherical nanoparticles or fine nanorods of ZnO consisting principally of tetra pod like structures are obtained selectively depending on the process parameters. Intermediate structures can also be synthesized. Trans-mission electron microscopy of the particles and rods shows that these are single crystals with diameters in the 5-50nm range. We find that the tetrapods have high absorption in the UV and nearly 100% reflectivity in the visible. UV absorption coefficients for suspensions of tetrapods are found to be substantially higher (x10) than for commercial nanocrystalline powders.

Keywords: ZnO, nanoparticlea, nanorods, tetrapos, nanospheres, TEM, UV absorption, Raman spectroscopy

1 INTRODUCTION

Due to its tunable electrical properties and stable chemical structure, zinc oxide has been used in varistor and sensor applications. High purity nano-crystalline ZnO with controlled particle size is used in medicine and cosmetic industry for transparent UV screens since it absorbs both UV A and UV B and has a low photo catalytic activity when compared to TiO_2 [1-3]. To ensure high absorption coefficients and transparency, the development of scaleable synthetic procedures that allow the large scale preparation of size and shape controlled ZnO is necessary. While solution methods suffer from the disadvantages of being laborious and susceptible to contamination by anions or organic additives, the gas phase chemistry has the advantage of producing high purity crystalline products in a single step reaction and is often preferred due to its lower cost [4,5]. Aerosol processes are increasingly being used for the large scale production of metal and oxide nanoparticles [6]. Various precursors have been used for the gas phase synthesis of ZnO that include Zn metal, diethyl zinc and more recently, organometallic precursors such as heterocubane [7-9]. In this com-munication we report the gas phase synthesis of high purity, nanocrystalline and non agglomerated spheres and rods of ZnO produced via a one step gas to particle conversion in an aerosol using zinc metal as the source. We find that spherical or rod shaped particles can be produced selectively in the aerosol by controlling the temperature of zinc vapor and that of oxidation.

2 EXPERIMENTAL

The reactor used was a 60 cm long tubular quartz gas flow reactor (Figure 1). All experiments were performed under atmospheric pressure. Zinc metal powder (325 mesh size) contained in an alumina boat was introduced in the central zone of the three zone furnace maintained under flowing Ar/N_2.

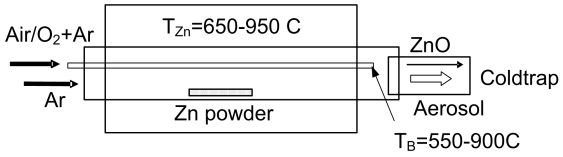

Figure 1. Schematic diagram of the reactor used for the synthesis.

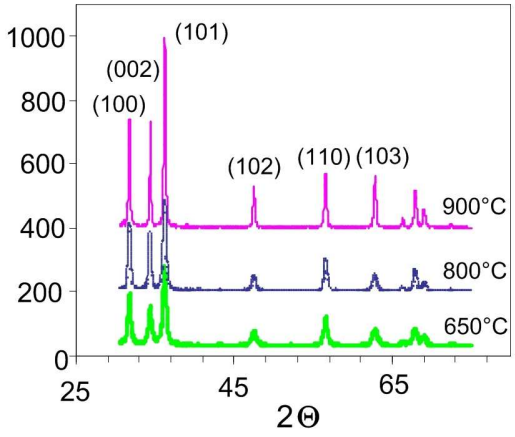

Figure 2. X-ray powder diffractogram of the nano-particles produced at Zn temperatures of 650, 800 and 900ºC.

A mixture of air/oxygen +Ar (in the ratio 1:1) in parallel or cross flow is introduced so as to react with Zn vapour at the point B. Zn temperature was varies from 650-900°C and

NSTI-Nanotech 2008, www.nsti.org, ISBN 978-1-4200-8503-7 Vol. 1

T_B was varied from 550-900C. The residence time of the zinc vapour was also varied by moving the point B. The Zinc vapor oxidized giving rise thick white fumes or fluffy particles that were collected at the cold end using liquid nitrogen traps. The rate of reaction depended principally on the oxidation temperature. The yield varied from 10 to 50% increasing with increasing oxidation temperatures from 550-900C. The fluffy white material was collected and characterized without further treatment.

3 STRUCTURE AND OPTICAL PROPERTIES

X-ray powder diffractograms of as produced material showed the crystalline phase of wurtzite structure for all temperatures. No preferred orientation was observed (Fig. 2). BET surface areas measured from nitrogen adsorption isotherms showed values ranging from 14 to 28m^2/g depending on temperature and morphology with tetrapods showing the highest value and are comparable to those for commercial samples (Degussa ADNANO20) (Fig. 3).

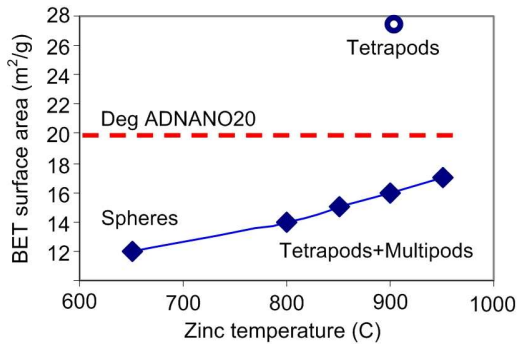

Figure 3. BET surface area as a function of synthesis temperature compared to the SSA for Degussa ADNANO 20.

Figure 4 shows electron micrographs of 4a), 4b) nanospheres and 4c), 4d) nanorods produced at T_{Zn} =650C and 900°C respectively. At 650ºC, the ZnO sample consists of nanoparticles with an average size of 26 nm. The average size was measured from over a hundred randomly selected particles. The smaller particles are spherical whereas the larger ones are faceted. At T=900°C, nanorods with length over 1 μm and with maximum diameter of 50 nm are obtained. Intermediate structures can also be synthesized. In contrast, the CVD ZnO collected from the reactor walls shows a mixture of morphologies for all the temperatures showing that the gas phase nucleation permits a better shape control. The atomic ratios of zinc and oxygen are calculated from EDX spectra to be approximately equal to 1. High resolution TEM showed that the spheres and rods are single crystals. The rods consist mostly of tetrapod type structures but also contain multipod type structures consisting of rods growing outward from plates of ZnO and there is no abrupt change in growth direction. For the tetrapods, there is no correlation between the growth direction of the four legs. The aspect ratios for the rods vary between 10 and 500 and the narrowest of them are around 5-8 nm in width.

The optical absorption spectra for colloidal solutions of ZnO particles and rods in ethanol are shown in Figure 5. All the dispersions are found to be stable for 24 h after sonication for 5 minutes in an ultrasonic bath. The absorption maximum varies from 366 nm for nanoparticles to 371 nm for the rods. In all cases, a shoulder is observed at 358 nm.

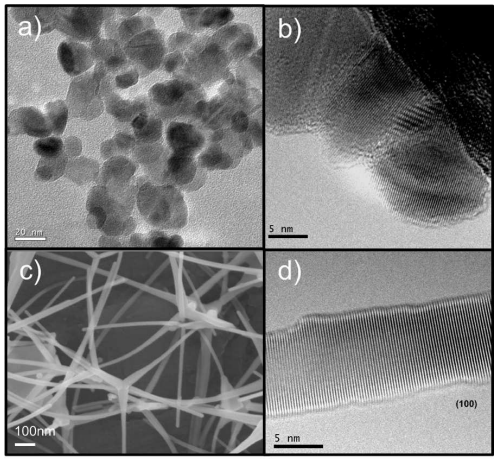

Figure 4. Electron microscopy images of ZnO nanospheres and tertrapods synthesized by CVS at two different temperatures: a) and b) T_{Zn}=650C, T_B=550C, c) and d) T_{Zn}=900C,T_B= 900C.

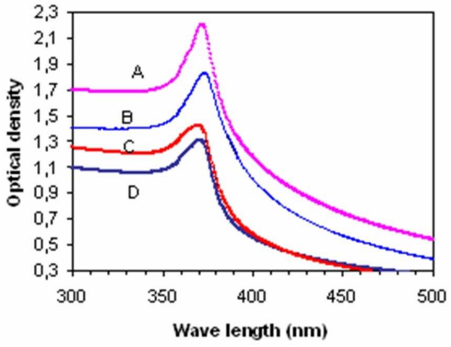

Figure 5. Optical absorption spectra of ZnO colloids A) nanorods, B) intermediate structures, C) nanoparticles and D) Degussa AD Nano 20 in ethanol (0.1mg/mL).

This shoulder is more pronounced for the nanoparticles and for Degussa ZnO than for the nanorods. The shoulder at 358nm is attributed to exciton absorption and is blue shifted with respect to bulk ZnO (380 nm) due to the small size of the colloids. Spanhel and Anderson [10] have measured the exciton spectra of ZnO colloids as a function of the

aggregate size. According to this study, absorption at 358nm corresponds to a size of around 5.8 nm that corresponds to the lowest observed aggregate size of our nanoparticles. The band at 275 nm observed by Spanhel et al is absent in our case showing the absence of smaller aggregates. The absorption at 370 nm corresponds to the band edge absorption. For the same concentration, the absorption coefficients are higher for the nanorods by one order of magnitude when compared to spheres showing the influence of shape on the UV absorption efficiency of nanocrystalline ZnO.

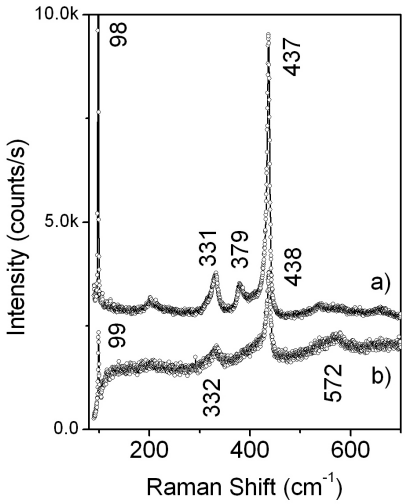

Figure 6. Raman spectra recorded at 632 nm of Zn nanorods (a) and Zn nanospheres (b).

The Raman spectrum of the ZnO nanorods in figure 6.a shows an intense peak at 437cm^{-1} corresponding to the high energy non-polar E_2 mode involving the oxygen sublattice. This band is at the same spectral position as in bulk ZnO. A less intense band is observed at 331cm^{-1} which is attributed to disorder induced second order scattering as has been reported for quantum dots of ZnO [11]. The band at 379 cm^{-1} can be assigned to the polar A_1 (TO) mode and we find in the spectral region of the A_1 (LO) mode at 572 cm^{-1}, a broad band. The intense and narrow (2 cm^{-1}) low energy non-polar E_2 mode of the Zn sublattice is observed at 98 cm^{-1}, slightly down shifted in energy from bulk ZnO (102 cm^{-1}). Figure 6.b shows spectra for nanospheres. The spectral bands are less intense with spectra differences in the region between the A_1 (TO) band at 379 cm^{-1} and E_2 band at 437cm^{-1} and A_1 (LO) band at 572 cm^{-1}. It is not clear at this stage whether a new band emerges between the A_1 (TO) and E_2 band or the E_2 band is asymmetric due to electronic coupling due to mobile charges. This indicates structural differences between nanorods and nanospheres. Surface induced structural changes for nanospheres in the small size range are more important which can lead to dynamic fluctuations between different crystal orientations. The Raman spectrum shows clearly the formation of the wurzite structure for nano spheres and nanorods.

4 CONCLUSIONS

Our results show that a simple substrate-free gas phase oxidation permits the formation of nanoparticles in the form of spheres and rods even at high temperatures without the use of organic stabilizer or organometallic precursors. We assume that Zn vapor forms metal clusters that react instantaneously with oxygen in the mixing zone of oxygen and metal vapor to produce primary particles of zinc oxide in the gas phase that coalesce and aggregate to form larger particles. These particles are directed towards the collector by thermophoresis. Large agglomerates are not observed in this synthesis. Rods or spheres are formed depending on the temperature of oxidation. Intermediate forms are also observed. BET surface areas comparable to commercial nanocrystalline ZnO have been observed for these nanoobjects. The nanorods show ten times higher absorption for UV radiation when compared to commercial nanoscale ZnO powders and can thus function as efficient UV absorbers.

ACKNOWLEDGMENT

The authors thank L. Datas and Y. Thibaud for SEM and EDS analysis. Financial support from Agence Nationale de recherche (ANR Projet PRONANOX, ANR-05-RNMP-002) France is gratefully acknowledged.

REFERENCES

[1] A.C. Dodd, A.J. McKinley, M. Saunders, T. Tsuzuki, J. Nanopart. Res. 8 (2006) 43.
[2] Z.W. Pan, Z.R. Dai, Z.L. Wang, Science, 291 (2001) 1947.
[3] L. Vayssieres, N. Beerman, S. Lindquist, A. Hagfeldt, Chem. Mater. 13 (2001) 4365.
[4] K. Nakaso, K. Okuyama, M. Shimada, S.E. Pratsinis, Chem. Eng. Sci., 98 (2003) 3327.
[5] R. Bacsa, Y. Kihn, M. Verelst, J. Dexpert, W. Bacsa, P. Serp, Surf. Coat. Tech., 201 (2007) 9200.
[6] M. Height, L. Maedler, S. Pratsinis, Chem. Mater. 18 (2006) 572.
[7] S. Polarz, A. Roy, M. Merz, S. Halm, D. Schroder, L. Schneider, G. Bacher and M. Driess, Small, **2005**, 5, 540-552.
[8] N. Ramgir, D. Late, A. Bhise, M. More, I. Mulla, D. Joag, K. Vijayamohanan**,** J. Phys. Chem. B**,** 110 (2006**)** 18236.
[9] G. Shen, Y. Bando, D. Chen, B. Liu, C. Zhi, D. Golberg, J. Phys. Chem. B 110 (2006) 3973.
[10] L. Spanhel, M. Anderson, J. Am. Chem. Soc. 113 (1991) 2826.
[11] K.A. Alim, V.A. Fonoberov, A.A. Balandin, Appl. Phys. Lett. 86 (2005) 053103